2010 IEEE International Conference on Robotics and Automation
Anchorage Convention District
May 3-8, 2010, Anchorage, Alaska, USA

Haptics-enabled Teleoperation for Robot-assisted Tumor Localization

A. Talasaz, *Member, IEEE*, R.V. Patel, *Fellow, IEEE*, and M.D. Naish, *Member, IEEE*

Abstract— **This paper focuses on the problem of incorporating haptics-enabled teleoperation in minimally invasive tumor localization. Since the stiffness of a tumor is higher than that of the surrounding tissue, it can be identified as a hard nodule when palpated. Using a Tactile Sensing Instrument (TSI) developed at CSTAR, the distributed pressure profiles along the contacting surface can be measured during remote tissue palpation. The tumor can be detected by using a visualization software that creates a color contour map based on the magnitude of the pressure over the palpated area. The accuracy of this method depends on the uniformity of the force applied to the tissue. A haptics-enabled teleoperation system provides the surgeon with the opportunity to feel the interaction force between the instrument and tissue during Minimally Invasive Surgery (MIS). The objective of this research was to assess the feasibility of combining force feedback with tactile feedback in order to increase the overall performance of tumor localization. The teleoperation system used in this work consists of a Mitsubishi PA10 robot as the slave that is remotely controlled (over a dedicated network) through a 7 Degree-Of-Freedom (DOF) haptic interface. A two-channel architecture, along with hybrid impedance control was utilized to form a bilateral teleoperation system in which the master is under force control and the slave is under position control. The experimental results confirm the effectiveness of using force feedback in robot-assisted tactile sensing for tumor detection.**

I. Introduction

Minimally invasive surgery, also called laparoscopic surgery, utilizes thin instruments and an endoscope to perform surgery through small incisions on the patient's body. This method has many advantages to both patients and healthcare system, including a reduction of surgical trauma and damage to healthy tissue, faster recovery times and shorter hospital stays. Robot-assisted surgery [1] is a specialized form of minimally invasive surgery that gives surgeons better vision, maneuverability and control than is possible with standard laparoscopy. This kind of surgery is usually performed as a form of teleoperation, defined as the remote control of a robot manipulator by a human operator via a control interface. Two types of manipulation can be done in teleoperation: unilateral teleoperation where the master unit only communicates with the slave robot and no information is sent back to the master, and bilateral teleoperation in which the master unit has the capability of force reflection and allows the surgeon to feel the interaction between the remote robot and its environment. This feeling, also referred to as haptics, can be in the form of force feedback or tactile feedback. Force feedback is the sensation of weight and resistance and allows the surgeon to feel the weight of remote objects or the resistance to motion, while tactile feedback includes the sensation of shapes and textures [2], or distributed properties acting on the contact surface. Two commercial robotic teleoperation systems for MIS are the da Vinci and the Zeus (no longer available), both from Intuitive Surgical, Sunnyvale, CA, U.S.A. In these systems, the surgeon controls the slave robotic arms that hold the surgical instruments through the use of master manipulators mounted at the surgeon's console. While these robots offer superior dexterity and position control, they both lack the ability to reflect forces. The force reflection capability in master-slave systems [3] is an important issue and the lack of force feedback in robotic surgery can be considered to be a safety risk because it can lead to accidental tissue damage.

Tumor localization is an important first step in tumor treatment [4], [5]. A number of techniques are available for detecting tumors; however, most of them suffer from disadvantages for use in minimally invasive surgery. Magnetic Resonance Imaging (MRI) and Computed Tomography (CT) for preoperative detection may not be useful during minimally invasive surgery because of tissue shift caused by insufflation of the abdomen or chest. Laparoscopic ultrasound can be used during MIS but for some applications like lung cancer surgery in which the diseased lung is collapsed, artifacts caused by residual air make it difficult to use, particularly when trying to localize small tumors (less than 1 cm diameter). Since the stiffness of a tumor is higher than surrounding area, one possible approach is to use tactile feedback to monitor pressure distribution where the highest value indicates a tumor. A industrial TactArray sensor from Pressure Profile Systems Inc. (PPS) was incorporated into a surgical probe suitable for MIS [6], [7]. Using this tactile sensing instrument (TSI), the tissue can be palpated manually or using a robot [4]. The most important issue here is how well the exploration force can be controlled by the user. Human palpation may lead to unreliable results due to the inconsistency in the amount of force applied to the tissue. When insufficient forces are applied on the tissue, artifacts in the image make it difficult to distinguish the tumor location. The application of a preprogrammed robot-assisted method is also limited because of the prior information needed for

This research was supported by the Ontario Centers of Excellence under grant IC50272, and the Natural Sciences and Engineering Research Council (NSERC) of Canada under Grant CRDPJ349675-06.

A. Talasaz is with CSTAR, Lawson Health Research Institute, London, ON, Canada and with the Department of Electrical and Computer Engineering, UWO, London, ON, Canada (email: atalasaz@uwo.ca). R.V. Patel is with CSTAR, the Department of Electrical and Computer Engineering and the Department of Surgery, UWO (phone: 519-685-8500 ext. 36618, email: rajni.patel@lhsc.on.ca). M.D. Naish is with CSTAR, the Department of Mechanical and Materials Engineering, and the Department of Electrical and Computer Engineering, UWO (email: mnaish@uwo.ca).

each tissue [5].

As a remedy for the aforementioned limitations, this paper present a data fusion method utilizing both tactile and force feedback. Tactile feedback is presented in a visual form to demonstrate the pressure distribution on the palpated area, while the force feedback is reflected to the surgeon's hand during MIS. By using this data fusion technique, the surgeon can better determine the exact location of the tumor based on provided visual clues and the extra force reflected to his/her hand when the tactile sensor touches a tumor. A two-channel bilateral teleoperation system [8] was used in this research consisting of the haptic wand as the master with capability of force reflection in 7 DOF [9] and Mitsubish PA10-7C as the slave. The hybrid impedance control technique [10] is used to control the behavior of robot manipulators when the tactile probe is in contact with the tissue.

The outline of this paper is as follows. First, tactile sensing for tumor detection is described briefly, and the bilateral teleoperation control method is then presented. The master-slave testbed is introduced in Section IV, and Section V describes the hybrid impedance control scheme. In order to implement bilateral control, a hand force observer is used which is described in Section VI. Experimental results are presented in Section VII, and Section VIII concludes the paper.

II. Tactile Sensing Tumor Detection

The tactile sensor array used in this research is a PPS TactArray developed to measure tactile pressure distribution of objects in direct physical contact with the. The sensor is attached to a surgical probe that has the appropriate dimensions for minimally invasive surgery [2]. The tactile data obtained from the sensor contains information about the magnitudes, distributions and locations of forces. Sapphire® real-time acquisition and visualization software and the PPS driver were used to visualize the pressure distribution. This real-time pressure profiling system converts the measured voltage values from the capacitive elements to pressure measurements, and displays these results in a color contour map of pressure distributions. Fig. 1 shows a screenshot of the pressure distribution produced by the software when a tumor is detected. As can be seen, this software utilizes the visual color spectrum to indicate the levels of localized pressure intensity experienced by the probe, with pink indicating the highest pressure intensity and blue indicating the lowest pressure intensity. Since the tumor is stiffer than the surrounding tissue, a tumor may be distinguished from the surrounding tissue by the highest pressure area indicated by pink color in contour map.

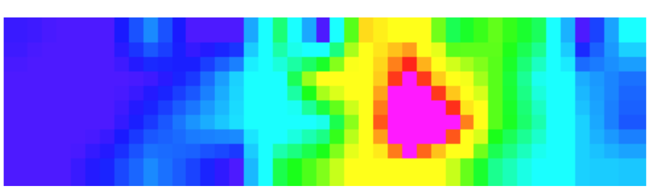

Fig. 1. Pressure distribution diagram obtained from visualization software.

III. Bilateral Teleoperation Control

Bilateral control architectures are classified by the number of communication channels required for transmitting position and force from the master to the slave and vice versa. Three architectures have been used for bilateral teleoperation; two-channel, three-channel [11] and four-channel control architecture [8]. The two-channel bilateral control architecture is most commonly found in the literature. This architecture has itself different configurations depending on the kind of signals that are being exchanged between the master and the slave. Among them, the most common two-channel architecture is a position-force architecture that allows the user to feel the slave's contact with the environment. In this control structure, the command position imposed by the operator is fed forward from the master as input to the position-controlled slave, and the interaction force between the remote slave robot and its environment is fed back as input to the force-controlled master. Fig. 2 depicts the two-channel bilateral teleoperation architecture.

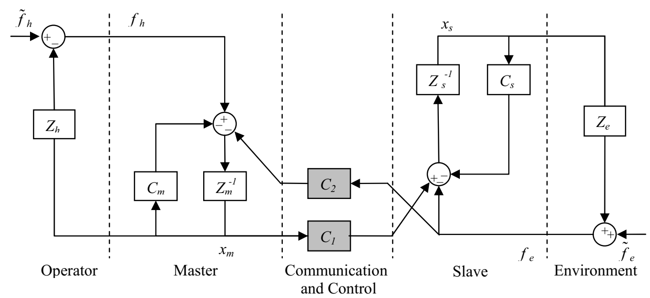

Fig. 2. The block diagram of two channel bilateral teleoperation.

In Fig. 2, $\tilde{f}_h$ and $\tilde{f}_e$ represent the operator's and the environment's exogenous input forces, which are independent of the teleoperation system behavior. The hand/master and the slave/environment interactions (force or torque) are denoted by f_h and f_e. The positions x_m and x_s denote the master and slave positions. The impedances Z_h, Z_m, Z_s and Z_e represent the dynamic characteristics of the operator's hand, the master robot, the slave robot and the remote environment. C_m and C_s denote the local position controllers and C_1 and C_2 are the two communication channels including coupling control for position forward and force backward, respectively.

IV. Master-Slave Testbed

Fig. 3 shows the master-slave testbed. It consists of a Mitsubishi PA10-7C robot as the slave and a customized Quanser Haptic Wand [12] as the master interface. The haptic interface used in the test-bed is a 7-DOF haptic device enhanced at CSTAR [9] from Quanser's 5-DOF Haptic Wand and is capable of position and force reflection in three translational DOF, three rotational DOF, in addition to grasping motion (Fig. 3, left). The haptic device workspace and the

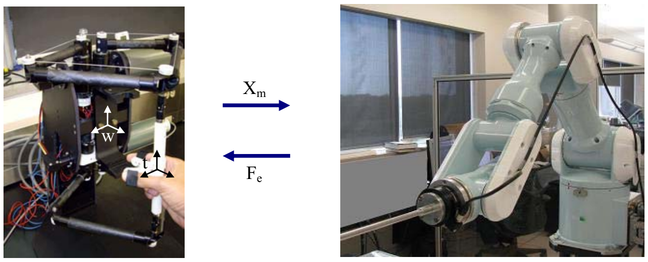

Fig. 3. Master-slave testbed: Left) Haptic wand, Right) Mitsubishi PA10 robot.

maximum continuous force/torques along the translational and orientational directions at the operating position are summarized in Table I. A 7-DOF Mitsubishi PA10-7C robot was also employed as the slave in the teleoperation test-bed (Fig. 3, right). The four-layer control architecture consists of the host control computer, a motion control card, a servo controller and the robotic arm. The host computer controls the robot and sends data packets via the ARCNET protocol to the servo controller at a sampling rate of 1 kHz. An ATI Gamma six-DOF force/torque sensor is attached to the robot wrist to measure the force exerted by the end effector on the tissue. The force resolution of this sensor is 0.0125 N in x and y directions and 0.025 N in z direction and the torque resolution is 1 mNm in all directions.

TABLE I
HAPTIC WAND CHARACTERISTICS

Haptic Wand Workspace	
Translation (mm)	480W x 450H x 250D
Rotation (deg)	±85 (roll) ±65 (pitch) ±160 (yaw) 30 (grasp)
Maximum Force/Torque	
Force (N)	2.3 (X) 2.1 (Y) 3.0 (Z)
Torque (N.mm)	230 (roll) 250 (pitch) 113 (yaw) 113 (grasp)

V. HYBRID IMPEDANCE CONTROL

In order to control the manipulator behavior when in contact with tissue, the Jacobian transpose Hybrid Impedance Control (JT-HIC) scheme was implemented for both the haptic wand and the Mitsubishi PA10-7C robot [10]. In this approach, the dynamics of the robot's interaction are modeled in terms of a mass-spring-damper. The Jacobian transpose based control scheme uses a task-space controller with damping terms. This controller attempts to generate a reference acceleration trajectory reflecting the desired impedance along the position-controlled subspace, and desired forces along the force-controlled subspace. This control method tries to regulate the force F_e while the robot is moving along a trajectory on the surface of the environment. Equations (1) and (2) show the reference acceleration trajectory for position and orientation subspace, respectively;

$$\ddot{X}_r = M_d^{p^{-1}}[-F_e + (I - S^p)F_d - B_d^p(\dot{X}_r - S^p\dot{X}_d) - K_d^p S^p(X_r - X_d))] + S^p\ddot{X}_d \qquad (1)$$

$$\dot{\omega}_r = M_d^{o^{-1}}[-\tau_e + (I - S^o)\tau_d - B_d^o(\omega_r - S^o\omega_d) - K_d^o S^o e_o^{rd})] + S^o\dot{\omega}_d \qquad (2)$$

and

$$X_r(0) = X(0)\,,\ \dot{X}_r(0) = \dot{X}(0),\ \omega_r(0) = \omega(0), \qquad (3)$$

where the superscripts p and o represent the position and orientation subspaces; M_d and B_d denote the desired mass and damping parameters; F_d and F_e are the desired force and environment contact forces; τ_d and τ_e are the desired torque and environment contact torques; The matrix S denotes the selection matrix that defines the force- and position-controlled subspaces ($S = I$ for entirely position-controlled and $S = 0$ for entirely force-controlled); X_d is a 3×1 vector that represents the desired Cartesian position, $\dot{X}_d$, and $\ddot{X}_d$ are the corresponding velocity and acceleration; ω_d and $\dot{\omega}_d$ represent the desired angular velocity and acceleration of the end-effector frame with respect to the base frame; e_o^{rd} is the orientation error between the desired orientation and the reference orientation.

Now, with the reference trajectory for both position and orientation, the objective is to design the control input τ such that the robot end-effector tracks precisely the obtained position and orientation trajectory. First of all, the position and orientation error between the robot end-effector and the reference trajectory needs to be calculated. The position error can be calculated as $e_p = X_r - X$, where X is the Cartesian position of the end-effector with respect to the base frame. The quaternion representation is used for the orientation of the robot. To quantify the error between the actual end-effector orientation and the reference orientation, the rotation error [13] is defined as $R_e \triangleq R_r R^T$, where R_r and R are the reference rotation matrix and the rotation matrix of the robot end effector, respectively. Now, let us assume the rotation matrix of the orientation to be:

$$R_e = \begin{bmatrix} \rho_{11} & \rho_{12} & \rho_{13} \\ \rho_{21} & \rho_{22} & \rho_{23} \\ \rho_{31} & \rho_{32} & \rho_{33} \end{bmatrix} \qquad (4)$$

In [13], it has been shown that the orientation error can be written as:

$$e_o = \frac{1}{2}\begin{bmatrix} \rho_{32} - \rho_{23} \\ \rho_{13} - \rho_{31} \\ \rho_{21} - \rho_{12} \end{bmatrix}, \qquad (5)$$

By computing the position and orientation error, the following control law can be chosen in the JT-AHIC scheme:

$$\tau = J^T\left((K_p + \frac{K_i}{s})\begin{bmatrix} e_p \\ e_o \end{bmatrix} + K_v\begin{bmatrix} \dot{e}_p \\ \omega_r - \omega \end{bmatrix}\right) - K_d\dot{q} + G(q), \qquad (6)$$

where J^T is the Jacobian transpose of the robot manipulator, K_p, K_i, and K_v are the proportional, integral and derivative gains of PID controller, respectively. ω_r and ω represent the reference and actual angular velocity. $K_d\dot{q}$ and $G(q)$ are also damping and gravity terms added to the control law in order to increase the performance of the controller.

VI. Hand Force Observer

To implement bilateral control method on master-slave system, the interaction force between the hand and the handle of the haptic device needs to be available. Since there is no force sensor attached to the haptic wand end effector to measure this force directly, a model-based inverse dynamics force observer [14] was used to estimate the external force applied by the hand.

An accurate dynamic model has been developed for the haptic wand in our previous work [9]. In general it may be assumed that the haptic wand has the following dynamics equation;

$$\begin{aligned} \tau + J^T F_{\text{ext}} &= M(\theta)\ddot{\theta} + V(\theta,\dot{\theta}) + G(\theta) + f(\theta,\dot{\theta}) \\ &= \tau_{\text{free}}, \end{aligned} \tag{7}$$

in which θ, $\dot{\theta}$, and $\ddot{\theta}$ are the joint angle, velocity, and acceleration vectors, τ and F_{ext} represent the vectors of actuator torque and the external force applied to the haptic wand, J is the robot Jacobian, M, V, G, and f denote the inertia matrix, Coriolis and centrifugal terms, gravity vector, and friction, respectively. τ_{free} is also defined as the required torque to move the robot in free space.

Then, the inverse dynamics force observer estimates the interaction forces at the robot end effector as:

$$\begin{aligned} \hat{F}_{\text{ext}} &= J^{-T}(M(\hat{\theta})\hat{\ddot{\theta}} + V(\hat{\theta},\hat{\dot{\theta}}) + G(\hat{\theta}) + f(\hat{\theta},\hat{\dot{\theta}}) - \hat{\tau}) \\ &= J^{-T}(\hat{\tau}_{\text{free}} - \hat{\tau}), \end{aligned} \tag{8}$$

where $\hat{\theta}$ is the joint angle vector measured by the encoders attached to the shaft of the motors. Velocities and accelerations are not directly measurable and are computed purely from joint angle measurements. But since differentiating the joint angles give extremely noisy results because of the slow motion of the haptic wand, we used a high-gain observer [15] to estimate $\hat{\dot{\theta}}$ and $\hat{\ddot{\theta}}$. The equations defining the high-gain observer for estimating $\hat{\dot{\theta}}$ are as follows:

$$\begin{aligned} \epsilon\dot{\hat{\theta}} &= \epsilon\hat{\dot{\theta}} + \alpha_1(\theta - \hat{\theta}) \\ \epsilon\dot{\hat{\dot{\theta}}} &= \alpha_2(\theta - \hat{\theta}), \end{aligned} \tag{9}$$

where ϵ is a small positive constant, α_1 and α_2 are chosen so that the roots of

$$s^2 + \alpha_1 s + \alpha_2 = 0 \tag{10}$$

have negative real parts.

Given $\hat{\theta}$, $\hat{\dot{\theta}}$, and $\hat{\ddot{\theta}}$, as well as an accurate dynamic model, $\hat{\tau}_{free}$ can be computed. The actuator torques are also calculated from the motor currents multiplied by the motor torque constants. Then, the interaction contact force can be estimated as indicated in (8).

VII. Experimental Results

To evaluate the effect of force feedback in robot-assisted tactile sensing for tumor localization, a master-slave haptic teleoperation was utilized to perform soft-tissue palpation. The tissue used for the experiments was *ex vivo* bovine liver obtained from a local store. An artificial 10 mm diameter hemispherical tumor made from thermoplastic adhesive (hot-melt glue) with encased thin metal wires to ensure its visibility in the radiographic image used later to assess accuracy, was embedded in the underside of the liver [4]. In the experiments, the operator used the master to palpate the tissue using TSI through the slave. Fig. 4 shows the master-slave robotic setup palpating tissue. The

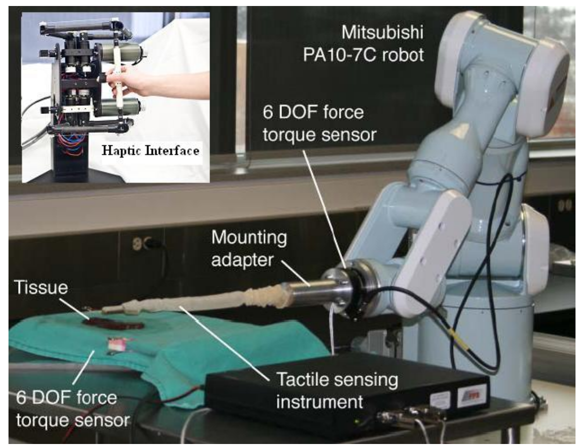

Fig. 4. Master-slave robotic setup palpating tissue.

implementation of the controllers was done on two Windows based systems, one for the master and the other for the slave. The communication between the two computers was done using the User Datagram Protocol (UDP) protocol. All control algorithms were implemented on the QuaRC Real-Time software which automatically generates real-time code directly from Simulink designed controllers targeting Windows and other operating systems [12]. Fig. 5 depicts the schematic diagram of the teleoperation system. All of the controllers for the master and slave manipulators were implemented at a sampling frequency of 1 kHz.

Fig. 6 also shows the block diagram of the two-channel position-force teleoperation architecture. Here, X_m is the position of the end effector of the haptic wand. The workspace of the haptic wand was mapped to the workspace of Mitsubishi PA10-7C robot by position scaling factor C_1. The scaled version of the operator's hand motion (through the haptic wand end effector) is the desired position command for the PA10 robot. On the other hand, the interaction force between the palpator mounted on the PA10 robot end effector and the tissue was measured by the ATI force sensor and generated a force F_e. This force was also scaled by the force scaling factor C_2. The scaled force is the desired force command of the force-controlled haptic wand.

The palpation was started from the home position of the PA10 robot with motion in an up and down direction cor-

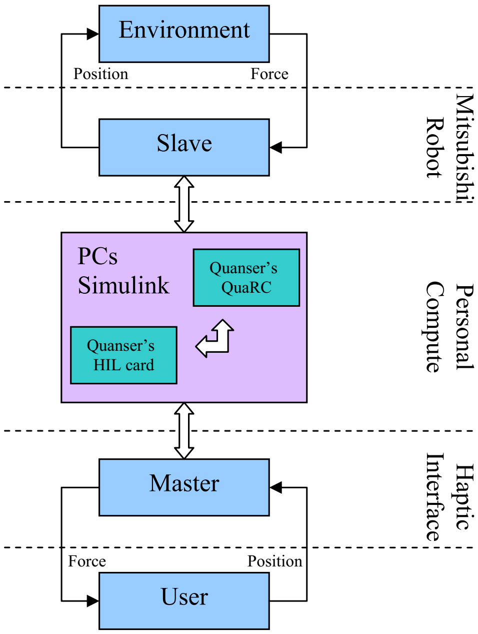

Fig. 5. Block diagram of the master-slave haptic teleoperation.

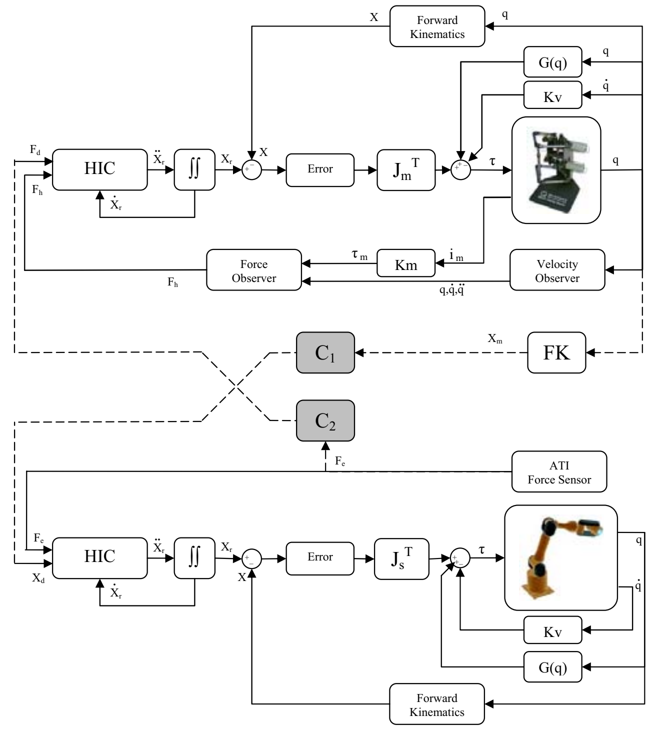

Fig. 6. The control system block diagram.

responding to the z-direction of the PA10 world coordinate frame and repeated for the other points along left-right direction (the y-direction of the PA10 world coordinate frame). When the PA10 robot palpated the tissue, the pressure map produced by the PPS software was saved and the interaction force between the tissue and the TSI was sent to the master side. In this experiment, eleven points along the y direction of the PA10 world coordinate frame were palpated (the length of the sensor almost covered the width of the tissue). Fig. 7 shows the pressure maps obtained for these points. As stated earlier, the pink color in the pressure map denotes the highest pressure in the palpated area. Using the pressure map results, one may conclude that there are four tumors inside the tissue while just one tumor was actually placed in the tissue. The haptics-enabled teleoperation results are presented in Figs. 8 and 9 ($C_1 = 0.5$ and $C_2 = 0.25$). As can be seen here, the position commands sent by the haptic wand were followed perfectly by the PA10 robot and the interaction force between the user's hand and the haptic wand handle estimated by the observer given in (8) precisely tracks the force applied to the tissue by the PA10 robot (There is a time difference between these two diagrams which is because of the priority in running the haptic wand as the server). The force diagram gives valuable information about the location of the tumor. As stated before, because of the higher stiffness that a tumor has, it can be distinguished from the surrounding area by more force being reflected to the user's hand during the palpation. Fig. 9 clearly demonstrates this phenomenon. The main advantage of this approach is that a surgeon can feel this extra force during minimally invasive surgery. Fig. 10 shows the data fusion for the obtained results; the force applied to the user's hand and the pressure distribution over

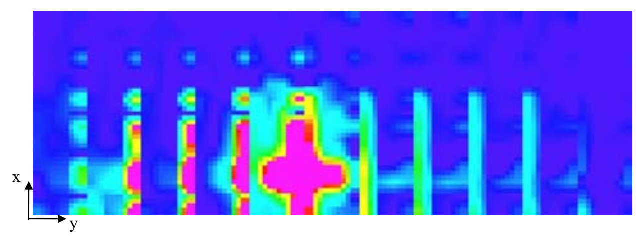

Fig. 7. Pressure map obtained from PPS software.

the contact area when the tissue was palpated. These results confirm that using the haptics information along with the tactile feedback in the visual form can significantly increase the accuracy of tumor detection. The average force applied to the user's hand during each palpation step is presented in Fig. 11 (marked as $*$). The curve fitted on the obtained results gives the best location of the tumor which is also confirmed by the results achieved by the pressure map. As can be seen, the force reflected to the user's hand when the tumor was palpated is twice the average force felt by the surrounding tissue.

VIII. Conclusion

The advantage of using haptics information during minimally invasive tumor localization was explored in this work. The current tactile sensing system for tumor detection is very sensitive to inconsistency in the amount of force applied to the tissue and may cause false positives for tumor detection because of artifacts in the resulting images. This work has shown that using haptics-enabled teleoperation system for

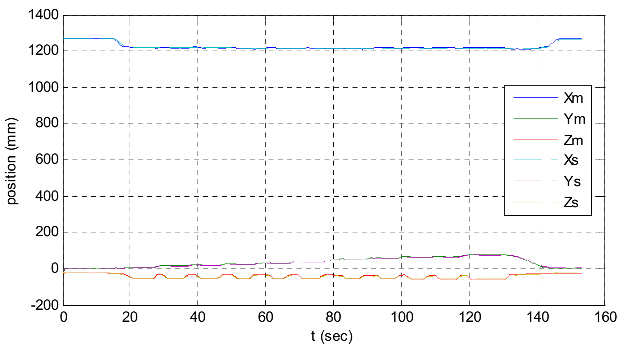

Fig. 8. The master-slave position tracking.

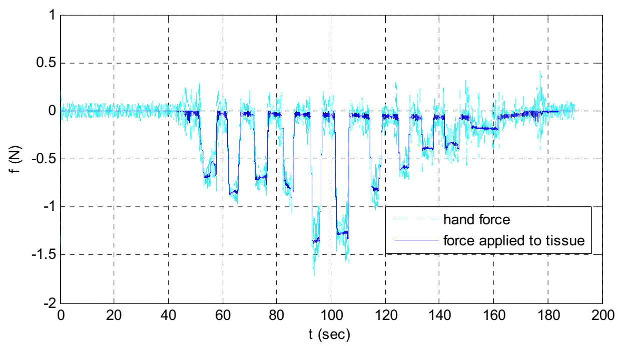

Fig. 9. The master-slave force tracking.

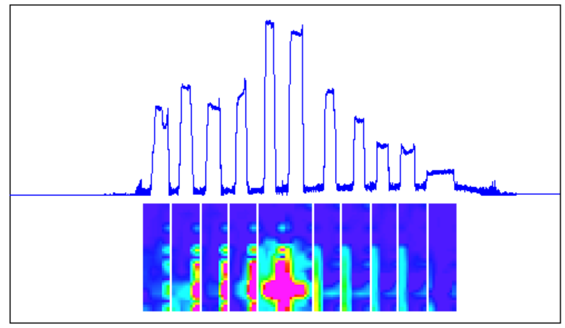

Fig. 10. The comparison between haptic results and visual tactile feedback.

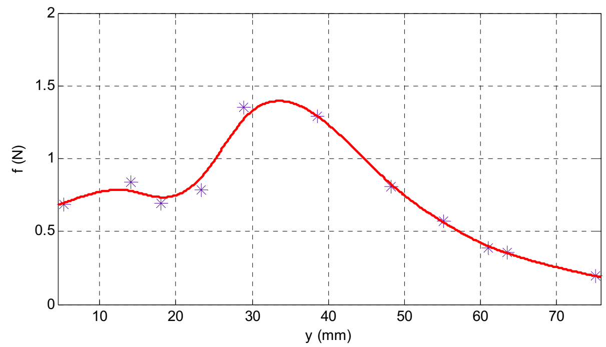

Fig. 11. The average force felt by the user during palpation.

tumor localization can not only enable a tumor to be detected via force reflection but can also increase the overall accuracy of detection. We see this approach as being used in conjunction with a modality such as tactile sensing to improve the reliability of the latter. From a practical perspective, for use in MIS, the presence of friction between the trocar and the palpation tool can affect the quality of the haptic interaction reported in this paper.

IX. Acknowledgments

The Tactile Sensing Instrument (TSI) used in the experimental work for this paper was designed at CSTAR in a project on palpation for minimally invasive surgery. The authors would like to acknowledge the contributions of Ana Luisa Trejos, Melissa Perri and Greig McCreery in the design, construction, calibration and validation of the TSI. The authors would also like to thank Jacob Apkarian, Ryan Leslie and Paul Karam of Quanser Consulting Inc. for help with the QuaRC software and the Haptic Wand.

References

[1] M. Tavakoli, R. Patel, M. Moallem, and A. Aziminejad, *Haptics-Based Systems for Robot-Assisted Surgery and Telesurgery: Design, Control, and Experimentation*. World Scientific Publishers in the series - New Frontiers in Robotics, 2008.

[2] M. V. Ottermo, M. Ovstedal, T. Lango, O. Stavdahl, Y. Yavuz, T. A. Johansen, and R. Marvik, "The role of tactile feedback in laparoscopic surgery," *Surgical Laparoscopy, Endoscopy and Percutaneous Technique*, vol. 16, no. 6, pp. 390–400, 2006.

[3] M. Tavakoli, R. V. Patel, and M. Moallem, "A force reflective master-slave system for minimally invasive surgery," in *IEEE/RSJ Conference on Intelligent Robots and Systems*, 2003, pp. 3077–3082.

[4] A. L. Trejos, J. Jayender, M. T. Perri, M. D. Naish, R. V. Patel, and R. Malthaner, "Robot-assisted tactile sensing for minimally invasive tumor localization," *The International Journal of Robotics Research*, vol. 28, no. 9, pp. 1118–1133, May 2009.

[5] G. L. McCreery, A. L. Trejos, M. D. Naish, R. V. Patel, and R. Malthaner, "Feasibility of locating tumors in lung via kinaesthetic feedback," *The International Journal of Medical Robotics and Computer Assisted Surgery*, vol. 4, pp. 58–68, Jan. 2008.

[6] R. S. Fearing, "Tactile sensing mechanisms," *The International Journal of Robotics Research*, vol. 9, no. 3, 1990.

[7] R. D. Howe, W. J. Peine, D. A. Kantarinis, and J. S. Son, "Remote palpation technology," *Engineering in Medicine and Biology Magazine*, vol. 14, no. 3, pp. 318–323, 1995.

[8] D. A. Lawrence, "Stability and transparency in bilateral teleoperation," *IEEE Transactions on Robotics and Automation*, vol. 9, no. 5, pp. 624–637, Oct. 1993.

[9] H. Bassan, A. Talasaz, and R. V. Patel, "Design and characterization of a 7-dof haptic interface for minimally invasive surgery test-bed," in *IEEE/RSJ Conference on Intelligent Robots and Systems*, Oct. 2009, pp. 4098–4103.

[10] R. Patel and F. Shadpey, *Control of redundant robot manipulators: theory and experiments*. Lecture Notes in Control and Information Science, Springer, 2005.

[11] K. Hashtrudi-Zaad and S. E. Salcudean, "Analysis and evaluation of stability and performance robustnes for teleoperation control architectures," in *IEEE International Conference on Robotics and Automation*, 2000, pp. 3107–3113.

[12] http://www.quanser.com. [Online]. Available: http://www.quanser.com

[13] J. Y. S. Luh, M. W. Walker, and R. P. Paul, "Resolved-acceleration control of mechanical manipulators," *IEEE Transactions on Automatic Control*, vol. AC-25, no. 3, pp. 468–474, June 1980.

[14] A. C. Smith, F. Mobasser, and K. Hashtrudi-Zaad, "Neural-network-based contact force observers for haptic applications," *IEEE Transactions on Robotics*, vol. 22, no. 6, pp. 1163–1175, Dec. 2006.

[15] H. Khalil, "Adaptive output feedback control of nonlinear systems represented by input-output models," *IEEE Transactions of Automatic Control*, vol. 41, pp. 177–188, Feb. 1996.